Experiment and simulation of dry particle coating

Akira Sato, Eric Serris, Philippe Grosseau, Gérard Thomas, Laurence Galet, Alain Chamayou, Michel Baron

Chemical Engineering Science, 2013, 86, 164-172, doi : 10.1016/j.ces.2012.07.037

Experiment and simulation of dry particle coating

AKIRA SATO[1, 2], ERIC SERRIS[3], PHILIPPE GROSSEAU[1], GERARD THOMAS[1], LAURENCE GALET*[2], ALAIN CHAMAYOU[2], MICHEL BARON[2]

[1] *Université de Toulouse, Mines-Albi, UMR CNRS 5203, Centre Rapsodee, Campus Jarlard, 81013 Albi, France*
[2] *Ecole Nationale Supérieure des Mines de Saint Etienne, Centre SPIN ; Département PROPICE ; LPMG - FRE CNRS 3312, 158 Cours Fauriel - 42023 Saint-Étienne Cedex 2, France*
[3] *Ecole Nationale Supérieure des Mines de Saint Etienne, Centre SPIN ; Département PRESSIC ; LPMG - FRE CNRS 3312, 158 Cours Fauriel - 42023 Saint-Étienne Cedex 2, France*

Abstract

The objective of this study is to get a better understanding of dry powder coating process using experiments and numerical methods. Materials chosen as host particles are SUGLETS® (granules mainly consisting of sugar) and as invited particles, magnesium stearate (MgSt). These two materials are introduced into a high shear mixer (Cyclomix). Operations were performed at various mixing time and rotation speed of the Cyclomix. The surface morphology analysis has confirmed that Suglet particles are coated with MgSt. The product properties such as flowability, wettability and particle size distributions were also characterized. The particle motion in the Cyclomix has been simulated by using Discrete Element Method (DEM). Both number of collisions and the collision force frequency are calculated. The simulation shows an increase of the collision number with the rotational speeds. This result indicates that choosing higher rotation speeds should be better for the dry coating process as long as the particles are not broken down.

Keywords:

Particle processing; Mixing; Dry coating; Numerical analysis; Simulation; Convective transport

I. Introduction

Dry particle coating is a method used to modify the properties of powders by attaching the fine particles (guest particles) onto the surface of core particles (host particles) by mechanical forces. As such neither aqua binder nor any organic solvents are required in the process. It is a simple process with low environmental impact and will receive considerable industrial attention. Even though a lot of experimental work on dry particle coating has been reported in the literature (Alonso et al., 1989, Honda et al., 1994, Watano et al., 2000, Ouabbas et al., 2009a, Lefevre et al., 2010 and Lefevre et al., 2011), the technique is not yet in commercial use. This is because the experiments are still in the trial and error state. In other words, it is difficult to predict the optimum operating conditions for commercial use and/or to scale up the process for industrial application. Few researchers have studied the theoretical

* Corresponding author : Laurence.Galet@mines-albi.fr

approaches for dry coating mechanisms with the aim of optimizing and improving the understanding of the process. For instance, Mei et al. (1997) developed an extended Johnson–Kendall–Roberts (JKR) particle model to include the effect of particle coating on the force–displacement relationship due to surface energy and elastic deformation. The method for determining the optimum operating conditions of equipment on dry coating processes based on the energy requirement for immobilizing the guest particles on the surface of host particles was also established (Iwasaki et al., 2002). The theoretical modeling of dry coating is a very important requirement for the optimization of the process and the design of new, more efficient apparatus geometries. However, this area of research is found to be less comprehensive. Hence, the objective of this study is to better understand dry powder coating by experimental and numerical methods. Since dry coating is generally achieved by mechanical forces, the particle motion would be the most important factor in determining the optimum operating conditions. Discrete Element Method (DEM), proposed by Cundall and Strack (1979), is one of the most popular techniques for simulating and analyzing the solid particle behavior and has been successfully applied in many fields (Kano et al., 1997, Matchett et al., 2000 and Cleary and Sawley, 2002). Thus DEM will be applied in this research to simulate the motion of the particles inside the coating apparatus. This research aims to reveal and hence describe the effect of operating conditions such as mixer rotation speed on particle coating, including a numerical approach.

II. Experiment

II.1. Materials

For the powders, Suglets and magnesium stearate (MgSt) were chosen as the host and guest particles, respectively. The Suglets were provided by NP Pharm Company. They are elliptical particles with a majority and minority composition of sucrose and maize starch, respectively. They have hydrophilic characteristics and are mainly used as an excipient in capsule and tablet formulation, particularly in multi-particulate systems. They can form cores upon which Active Pharmaceutical Ingredients (APIs) are coated for controlled or sustained release, drug delivery technologies. The use of such sugar spheres in multi-particulate drug delivery system is an area of increasing interest in the pharmaceutical industry. This is largely due to the clinical and formulation advantages sugar spheres have over single-unit dosage forms, including the ease of proceeding in modified release applications. An especially useful trait is that Suglets are able to withstand the process of drug layering (coating) an accurate amount of the API in the products. Fig. 1a shows a SEM image of Suglet particles. They are relatively elliptic shape and their surface seems to be angulated. The magnesium stearate (MgSt) guest particles are a fine, white, greasy, cohesive and hydrophobic powder widely used in pharmaceutical formulations as a lubricant. The shape of the MgSt is relatively random, including needle-like and plate-like configurations (Fig. 1b). Fig. 2 shows the particle size distributions of Suglets and MgSt obtained with a Malvern dry feed system (Mastersizer 2000). The volume distribution of Suglets shows one narrow population with median diameter (D50) about 250 μm. However, a wide size distribution is observed for MgSt. The size of MgSt particles varies from less than 1 μm–20 μm. The D50 for MgSt is about 4 μm. These properties of the samples are summarized in Table 1.

II.2. Coating process

A 1 L Cyclomix has been chosen to perform a dry coating in this study. This apparatus is defined as a high shear mixer/granulator, manufactured by Hosokawa Micron B.V. As seen from Fig. 3, the device consists of a conical vessel with an axial impeller in the centre equipped with four sets of specially designed blades. It applies high mechanical impact and shearing forces on the particles in order to break the guest agglomerates and coat them on the host particles. This device has previously been used successfully for dry particle coating experiments (Ouabbas et al., 2009b). The mass fraction of guest particles to host particles required in a coating experiment is calculated using a simplified model in order to guide the

experimental work. This model is based on the two following assumptions permitting a theoretical calculation: the guest and host particles have uniform sizes and are spherically shaped (even though in this case, the SEM images in Fig. 1 shows that they are not); and a 100% monolayer surface coverage of guest onto the host particles surface is achieved by the process. This mass ratio of guest to host particles, w can hence be expressed using the following equations (Thomas et al., 2009):

$$w = \frac{4C_{2D}(k_H+1)^2}{4C_{2D}(k_H+1)^2+\frac{\rho_H}{\rho_I}k_H{}^3} \quad (1)$$

$$k_H = \frac{R_H}{R_I} \quad (2)$$

where, k_H is the size ratio of host and guest particle, C_{2D} is the packing fraction of guest particles on the surface of the host particle, ρ_H and ρ_H are the densities of host and guest particles, respectively, and R_H and R_I are the radii of host and guest particle, respectively. Based on the assumption that the guest particles will pack on the surface in a compound hexagonal structure, C_{2D} can be estimated at 0.906. This gives an ideal mass ratio of around 3.92%. In this work, the mass ratio has been chosen as 5%. To focus on the effect of the operation time and rotational speeds, the mass of the host particles and the mass fraction was fixed for the duration of the study. The rotational speeds were in the range of 500–1500 rpm and the operation time was varied from 1 to 30 min. The operating conditions are given in Table 2.

II.3. Characterization

Various characterization methods were used to test the effects of dry particle coating. The surface morphology of the particles has been observed by scanning electron microscopy (SEM). In addition to the surface morphology the SEM enabled the identification of the guest particles on the host particle surface using Electron Dispersive X-ray (EDX) analysis. The Malvern Mastersizer 2000, as described previously, was used to measure the particle size distribution of the samples. The device also provided qualitative information regarding the interaction strength between host and guest particles by the way of recording the change in composite particle size over a range of dispersive air pressures. A Freeman technology powder rheometer (FT-4) was chosen to characterize the flowability of the products. This device analyses the Flow Rate Index (FRI), which represents the flowability of a powder; high FRI values are characteristic of cohesive powders. The sessile drop test was also completed to evaluate the wettability of the products.

III. Simulation of the particle motions in the mixer

The particle motion in the Cyclomix has been simulated by the discrete element method (DEM).

Fig. 4 shows the geometry of Cyclomix modeled for the DEM simulation. The host particles (with the properties detailed in Table 3) were simulated in the Cyclomix vessel using a hexagonal close packed structure. Gravity effects have been introduced as an external condition imposed on the assembly yet submitted on the forces developed by the rotating impellers. The current computer power is not enough to simulate the actual number of particles. As such a smaller number of particles (about 40,000) with larger size (2.0 mm) has been applied. To estimate the coating efficiency several values that could be related to the coating have been measured. These include the collision frequency, average rotational distance and the distribution of the collision forces. The average rotational distance shown in Eq. (3) could be especially very important for the coating. When the host particle rotates (Fig.

5), the guest particles near this host particle would stick to the surface and form a bigger particle.

$$\varphi_{avg} = \frac{\sum_{N}^{i=1} \varphi_i}{N} \quad (3)$$

IV. Result and discussion

IV.1. Surface morphology

The SEM images of the particle surface after the dry coating operation are shown in Fig. 6. For the particles coated at 500 rpm for 60 s, it can be seen that almost the entire surface of the particle is covered by MgSt. This might be because the experiments were carried out with powder quantities in excess of those defined by the ideal mass ratio. It is also possible that the adhesive forces between the host and guest particles may have been higher than expected. An increase in operating time caused the composite surface to become smooth. This could be because the MgSt deforms and creates a film-like coating under the high shear and impact forces. That is to say the dry coating process progressed from a dispersed coating to continuous film coating. At operating conditions of 1000 rpm for 60 s the coated product surface seemed rougher than that achieved at 500 rpm. At operating times of 600 s and 1800 s surface agglomeration was seen to be present. This was not solely guest particle agglomeration; flakes of the host particle were able to break off from the bulk and form an agglomerate before adhering back onto the host particle. This created a composite particle surface consisting of host particle flakes and MgSt. Operation for 60 s at 1500 rpm resulted in a surface similar to that produced by 1800 s at 500 rpm. After 600 s and 1800 s operation times the particle surface is seen to be comparable to that achieved at 1000 rpm for the same duration. To verify the attachment of MgSt to the Suglet surface, EDX analysis of elemental magnesium was conducted. The yellow spots shown in Fig. 7 indicate the presence of elemental magnesium across almost the entire particle surface, even though the appearance of the surface is flat.

IV.2. Flowability

The Flow Rate Index (FRI) value was measured after the dry coating treatment. Fig. 8 shows FRI as a function of operating time at each rotational speed. The initial value of FRI is that of the host particle. At 500 rpm, FRI decreases with an increasing operating time. In other words, the flowability of the composite is improving. In addition, the surface is getting smoother along with the operation time at 500 rpm as seen in Fig. 5. This could be the cause for the improved powder flowability. The same is observed for 1000 rpm operations, FRI decreases with an increase in the operation time. This decrease is faster for the 1000 rpm operation compared to the 500 rpm operation at operating times up to 300 s and above this the relationship is stable. At 1500 rpm, FRI decreases with an increase in the operation time up to just 60 s. After this it increases rapidly to a given value. This could be because of the fragmentation or breakage of the host particles due to the high shear stress and impaction forces that result from particle–particle and particle–wall/impeller interactions.

IV.3. Wettability

The water drop test has been carried out to analyze the wettability of the products. A small distilled water drop of 10 μl is deposited on the surface of a powder bed of the product. The contact angle of the drop is then measured after 30 s at room temperature. In addition, to avoid breaking the coating or particles themselves, the powder bed was handled with minimum compression; a spatula was used to create a homogenous, as flat as possible powder bed surface. The measurement of the contact angle was carried out three times and an average was calculated. Fig. 9 shows that the images of the water drop test for raw Suglets and for the product submitted to 1000 rpm for 60 s. As can be seen, the water drop has been absorbed as soon as it made contact with the powder bed due to the Suglets high hydrophilic properties.

On the other hand, the water drop on the coated product is still present after 30 s. It can be said that in terms of wettability the 60 s operation at 1000 rpm is enough to change the surface property from hydrophilic to hydrophobic. Fig. 10 shows the contact angle of the products as a function of the process conditions. The initial point of this figure is calculated and induced identically by the following equations.

$$\theta(t_0) = S_H\theta_H + (1 - S_H)\theta_I \quad (4)$$

$$S_H = \frac{{k_H}^2}{4C_{2D}(k_H + 1)^2 + {k_H}^2} \quad (5)$$

where, θ_H and θ_I are contact angles of host and guest particle, respectively, and S_H is the surface fraction of host particles. Since the contact angle of host particle θ_H and that of invited particles θ_I are 0° and 132°, respectively, the value of the contact angle of initial mixture, θ (t0) could be found as 104°. As seen in Fig. 10, at 500 rpm operating condition the contact angle increases with an increase of operation time until 300 s. Above this, it seems to become stable and the value is almost the same as that of MgSt, which indicates that the surface of the host particle is almost covered by the MgSt at 300 s operation. At 1000 rpm the contact angle increases more rapidly than that of 500 rpm up to 60 s operation, however, the contact angle decreases slightly with increased operation time after that. This might be because of the fragmentation or the breakage of the host particles. At 1500 rpm, it also increases up to 60 s operation, then, after this, it starts to decrease along with the operation time with more remarkable rapidity. That also might be due to the attrition of the host particles.

IV.4. Particle size distribution analysis

Volume distributions were analyzed using a Malvern Mastersizer 2000. Fig. 11 shows the volume distribution obtained with 2.5 bar dispersive air pressure at each rotational speed. At 500 rpm the majority of the products show as similar population to that of the Suglets. However, there are small populations of the products obtained from 60 s and 180 s treatments, which are similar to that of MgSt. This indicates that there is a small release of MgSt particles from the Suglet surface due to the air pressure (Fig. 11a). At 1000 rpm, on the other hand, there is no remarkable change observed (Fig. 11b). At 1500 rpm, there are the populations with sizes from 5 to 60 μm. These are probably small fragments of the Suglets and consequential aggregates (Fig. 11c). The number distribution shows these tendencies clearer. Fig. 12 shows the number distributions obtained with 2.5 bar air pressure. At 500 rpm, the populations of the products obtained from 60 s to 180 s are found to be around 7–8 μm, which are not fully corresponding to that of free MgSt (Fig. 12a). There are two possible explanations for this: (1) the populations are not a result of MgSt but are instead the result of fragmented Suglets; and (2) the populations are a result of MgSt released from the surface of the composite particles and which are subsequently deformed from the original MgSt shape and size. Since the products of longer operating times have been seen to have a Suglet population, the second explanation is more reasonable. At 1000 rpm, almost all the populations of products is that of Suglets, except for the product of 60 s operation. This tendency indicates that 1000 rpm operation gives stronger adhesion between host and guest particles than 500 rpm. At 1500 rpm, a different tendency was observed. The products obtained from 600 s and 1800 s operation times have populations around 60 μm. This is not seen from the products of the other rotation speeds. Considering these results are obtained from high speed rotation operation it can be assumed that the particle population diameter is caused by fragmentation of the Suglets.

IV.5. Numerical results

An example snapshot of the DEM simulation is shown in Fig. 13. The different colors show the velocity distribution of the particles. Blue particles have lower velocity and red ones higher velocity. The particles around the impeller exhibit higher velocities. There are few particles at

the bottom part of the vessel, which indicates that impellers force the particles to go along the wall and then, due to the effect of the conical shape wall, the particles travel upwards within the vessel. Finally, the particles around the vertical rotor shaft fall down to the bottom of the vessel. A convective movement of particles is thus observed.

The parameters that are related to the dry coating phenomena such as the number of collisions and the average rotational distance are shown in Fig. 14. The number of collisions increases with an increase in the rotational speed. It increases rapidly up to 1000 rpm, however, over 1000 rpm it increases moderately. The rotational distance increases linearly with an increase in the rotational speed up to 2500 rpm. Over 3000 rpm a small decrease is noted. That is because at high rotational speeds a large number of particles are forced to the top of the vessel and consequently less impact events between particles occur (even though there is high contact within the particle bulk). These results indicate that the dry coating efficiency increases when the rotational speed increases until a threshold value of the rotation speed. Fig. 15 shows the distribution of the colliding forces of the particles. The orders of forces range from 10−2 to 102 N. The peak height increases with an increase in the rotational speed. In the same time, the maximum forces increase too. This result indicates that the colliding forces increase with an increase in the rotational speed. Unfortunately, the yield stress of Suglets does not appear clearly in the literature. According to Colorcon (2009) data the breaking force of similar sugar spheres SureSpheres is from 4 to 7 N. The distribution of calculated colliding force given in Fig. 15 shows a value below this breaking force at low rotation speed. These observations are in accordance with the experimental data (Section 4.4) showing that no breakage or attrition occurred on Suglets at 500 rpm. However, at higher rotation speed the colliding forces are much higher and breakage or attrition were observed experimentally (1500 rpm).

So if the yield stress of the particles is input, it is reasonable to think that the breakage of the particles could be predicted by this approach.

IV.6. General discussion

All these characteristics evolutions can be used to propose the following evolution of the system during mixing (Fig. 16). Step (1) a discrete coating occurs rapidly, decreasing powder wettability to 132° and decreasing the FRI with increasing operating time and rotational speed. The collision number and rotational distance given by the DEM analysis agree with the characteristic changes qualitatively. The DEM analysis can provide a rough guideline to the optimum operating conditions. Step (2) a continuous film-like coating occurs and consequently the wettability and FRI value remain constant. This “pseudo-steady state” is reached for coating conditions such as 1000 rpm for 60 s–600 s of mixing. For rougher treatments (at 1500 rpm), step (3) occurs, the breakage and fragmentation of coated particles occurs as shown by PSD analysis. This results in increased wettability and FRI of the particles. As shown in Fig. 16, it is safe to assume that this breakage may open the coating film and generate “free” Suglet surfaces responsible for the drop of wettability from 132° to 110°. This is clear degradation of coating quality. The DEM analysis can estimate the impact forces of all collision events. It can therefore be used to suggest an optimum rotational speed to help prevent particle fragmentation and thus the degradation of coating quality.

V. Conclusion

In this study, dry coating experiments were carried out using a Cyclomix high shear mixer in order to coat Suglets with MgSt using different operating conditions. The particle characteristic evolution indicates that the guest particles initially cover the host particles discretely and then they deform to appear as a film-like coating. In addition attrition is induced by excessive operating conditions, which result in the worsening of dry coating performance. The flowability improves along with the mixing operation. However, this improvement is lost when breakage or abrasion of host particles occurs. Particle size distribution indicates the presence of the separation of the guest particles and breakage of the host particles. The DEM simulation of these experiments has been performed. The results

show that the dry coating performance improves with increased rotational speed until an asymptotic level. These results qualitatively agree with experimental measurement except for the stage of degradation of coating quality caused by excessive rotational speed. DEM can roughly suggest the optimum operating condition. Furthermore, development of this analysis requires more precise information in order to optimize the operating condition. Since the DEM analysis can give all the information of colliding events, this degradation stage induced by breakage of host particles could be predicted.

Nomenclature

C_{2D}	Packing fraction	[dimensionless]
D_{50}	Median diameter	[m]
E	Young's modulus	[GPa]
i	i-th particle	[dimensionless]
K_H	Size ratio of both host and guest particles	[dimensionless]
N	Number of particles	[dimensionless]
R_H	Radius of host particle	[m]
R_I	Radius of guest particle	[m]
S_H	Surface fraction of host particles	[dimensionless]
T	Total simulation time	[s]
w	Mass ratio of guest powders	[dimensionless]
θ_H	Contact angle of host powder	[°]
θ_I	Contact angle of guest powder	[°]
$\theta(t_o)$	Contact angle at initial point	[°]
ρ_H	Density of host particle	[kg/m^3]
ρ_I	Density of guest particle	[kg/m^3]
φ_{avg}	Average rotational distance	[m]
φ_i	Rotational distance of i-th particle	[m]
t	Time step of the simulation	[s]

References

M. Alonso, M. Satoh, K. Myanami, Mechanism of the combined coating—mechanofusion processing of powders, Powder Technol., 59 (1989), pp. 42–52

P.W. Cleary, M.L. Sawley, DEM modelling of industrial granular flows: 3D case studies and the effect of particle shape on hopper discharge, Appl. Math. Model., 26 (2002), pp. 89–111

www.colorcon.com/literature/marketing/ex/Surespheres/ex_ads_SureSpheres_Tech_Eval.pdf〉

P.A. Cundall, O.D.L. Strack, A discrete numerical model for granular assemblies, Geotechnique, 29 (1979), pp. 47–65

H. Honda, M. Kimura, F. Honda, T. Matsuno, M. Koishi, Preparation of monolayer particle coated powder by the dry impact blending process utilizing mechanochemical treatment, Colloid. Surface. A, 82 (1994), pp. 117–128

T. Iwasaki, M. Satoh, T. Ito, Determination of optimum operating conditions based on energy requirement for particle coating in a dry process, Powder Technol., 123 (2002), pp. 105–113

J. Kano, N. Chujo, F. Saito, A method for simulating three dimensional motion of balls under presence of powder in a tumbling mill, Adv. Powder Technol., 8 (1997), pp. 39–51

G. Lefevre, L. Galet., A. Chamayou, Dry coating of talc particles with fumed silica: influence of the silica concentration on the wettability and dispersibility of the composite particles, Powder Technol., 208 (2010), pp. 372–377

G. Lefevre, L. Galet, A. Chamayou, Dry coating of talc particles: effect of material and process modifications on their wettability and dispersibility, Am. Inst. Chem. Eng., 57 (2011), pp. 79–86

A.J. Matchett, T. Yanagida, Y. Okudaira, S. Kobayashi,Vibrating powder beds: a comparison of experimental and distinct element method simulated data, Powder Technol., 107 (2000), pp. 13–30
R. Mei, H. Shang, J.F. Klausner, E. Kallman, A contact mode for the effect of particle coating on improving the flowability of cohesive powders, Kona, 15 (1997), pp. 132–141
Y. Ouabbas, A. Chamayou, L. Galet, M. Baron, G. Thomas, P. Grosseau, B. Guilhot, Surface modification of silica particles by dry coating: characterization and powder ageing, Powder Technol., 190 (2009), pp. 200–209
Y. Ouabbas, J. Dodds, L. Galet, A. Chamayou, M. Baron, Particle-particle coating in a cyclomix impact mixer, Powder Technol., 189 (2009), pp. 245–252
G. Thomas, Y. Ouabbas, P. Grosseau, M. Baron, A. Chamayou, L. Galet, Modeling the mean interaction forces between powder particles. Application to silica gel-magnesium stearate mixtures, Appl. Surf. Sci., 255 (2009), pp. 7500–7507
S. Watano, Y. Imada, K. Miyanami, C.Y. Wu, R.N. Dave, R. Pfeffer, T. Yoshida, Surface modification of food fiber by dry particle coating, J. Chem. Eng. Jpn., 33 (2000), pp. 848–854

Tables

Table 1: *Properties of Suglets and magnesium stearate particles.*

Particles	D_{50} (µm)	Density (kg/m³)	Water interaction
Suglets	250	1580	Hydrophilic
MgSt	4	1140	Hydrophobic

Table 2: Operating conditions.

Coating device	Rotation speed (rpm)	Time (s)	Mass % of MgSt
Cyclomix	500, 1000, 1500	60–1800	5%

Table 3: Parameters for simulation.

Young's modulus E (GPa)	4.5
Poisson's ratio	0.30
Density (kg/m³)	160
Coefficient of restitution	0.16
Time step t (s)	2.0×10^{-6}
Total simulation time T (s)	1.5

Figures

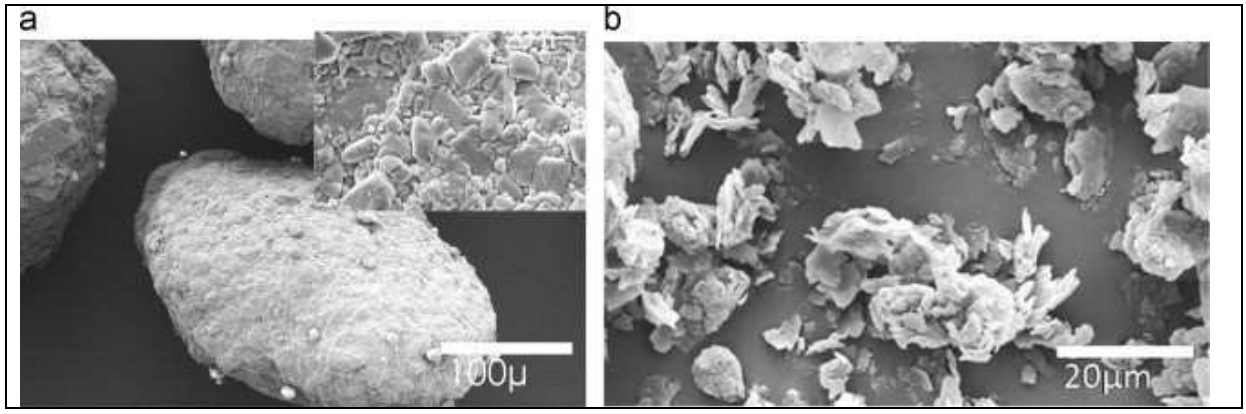

Figure 1: SEM images of Suglets (a) and MgSt (b).

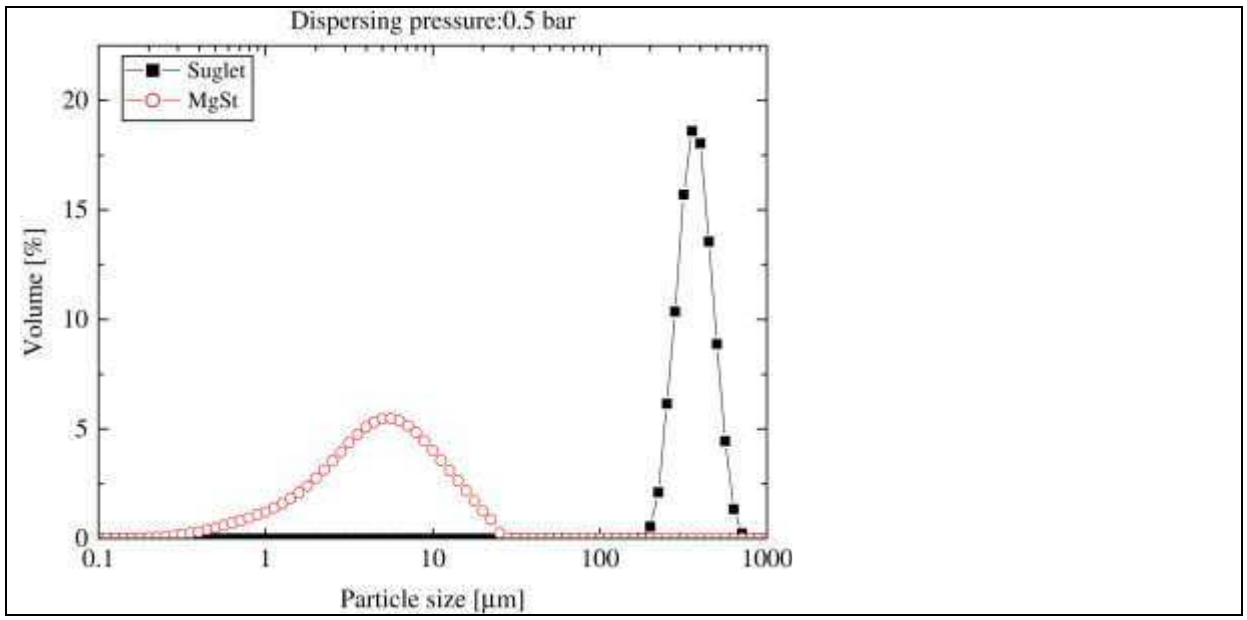

Figure 2: Particle size distributions of host (Suglets) and guest (MgSt) particles.

Figure 3: Cyclomix high shear mixer lab-scale device.

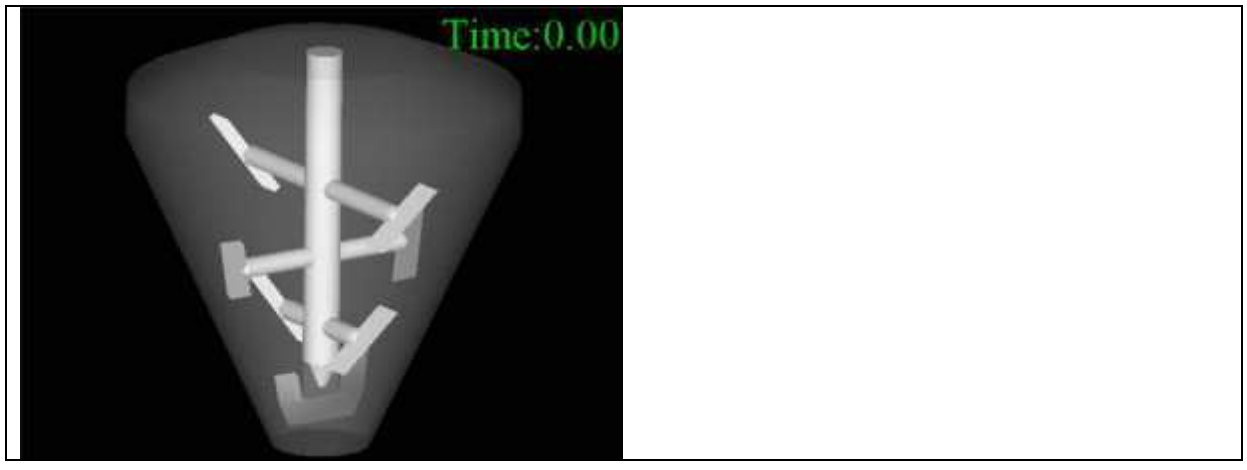

Figure 4: The geometry of the modeled Cyclomix.

Figure 5: Definition of rotational distance of the i-th particle.

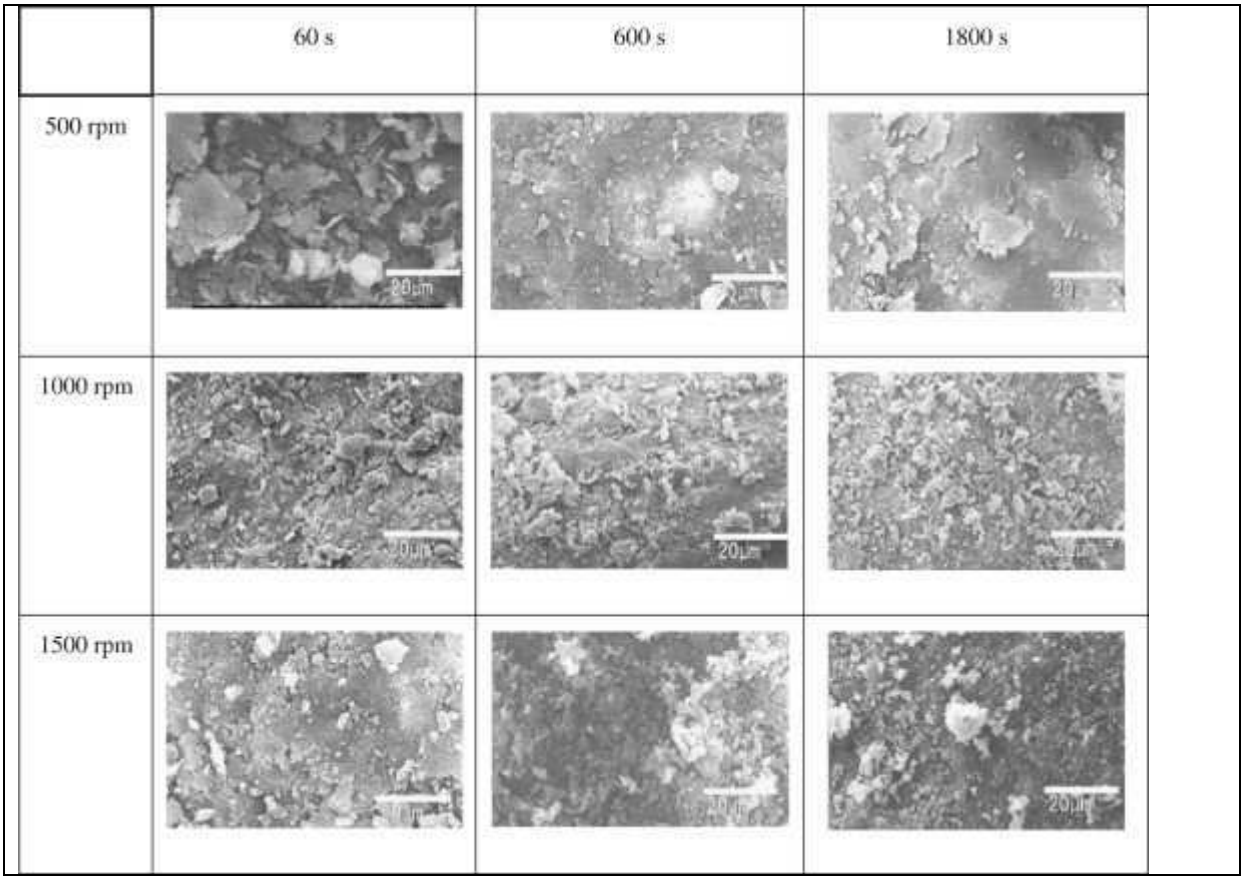

Figure 6: SEM images of the composites' surface after each operation

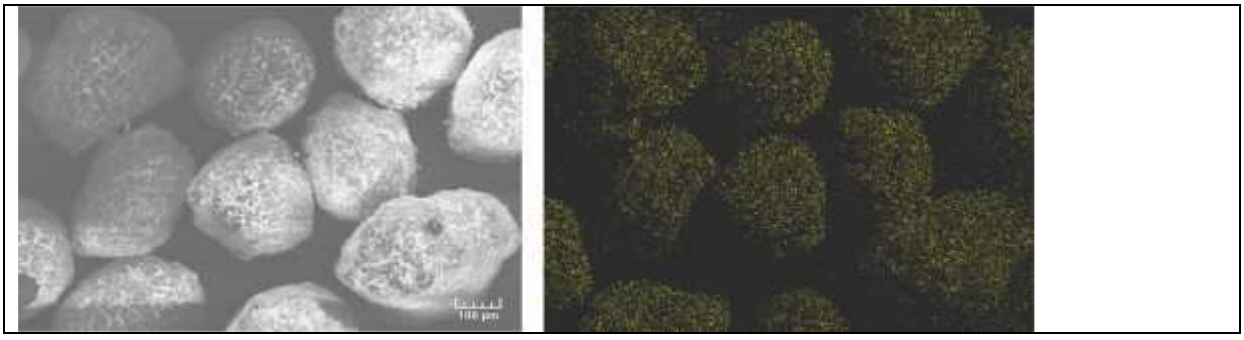

Figure 7: SEM images of composite (600 s at 500 rpm) and its EDX analysis of Mg element.

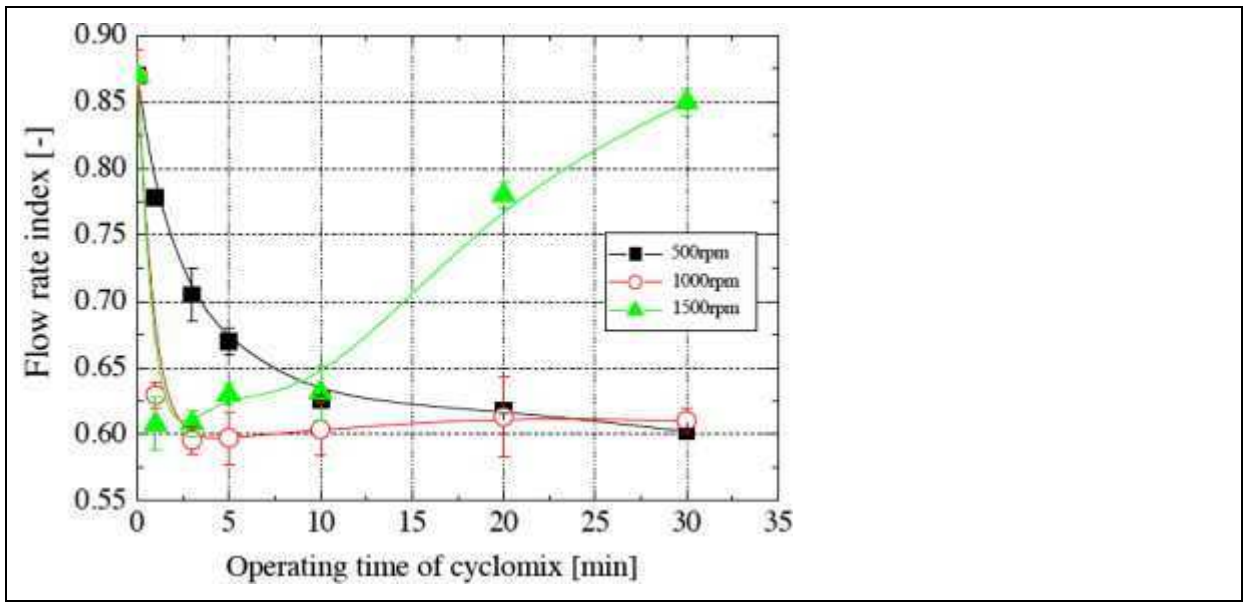

Figure 8: Flow rate index (FRI) as a function of operating time

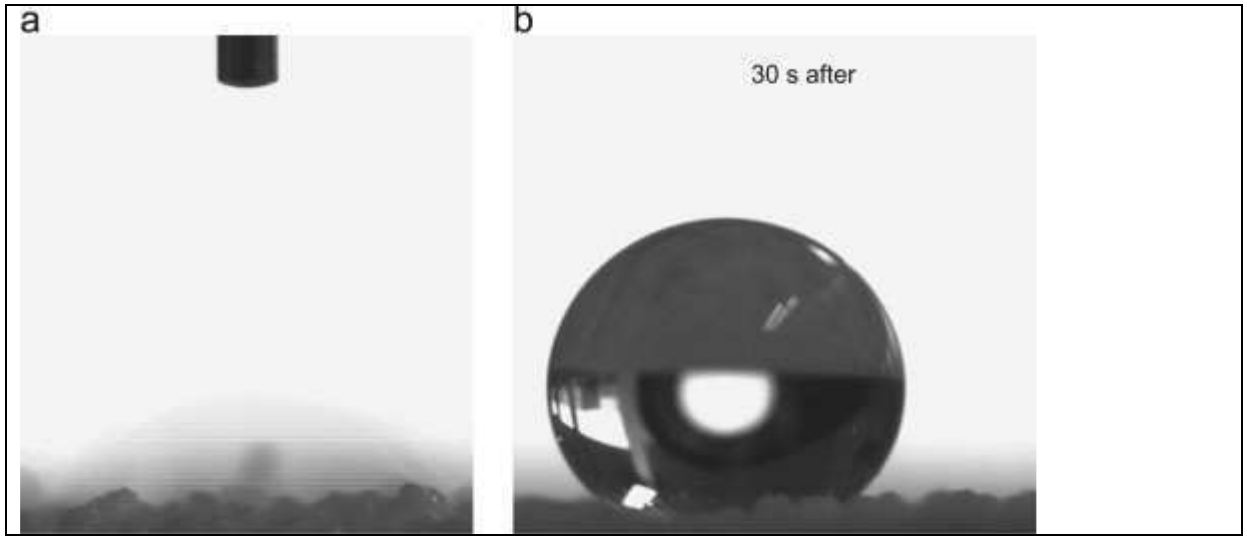

Figure 9: Images of the water drop test, (a) raw Suglets, and (b) Suglet+5% MgSt 60 s at 1000 rpm.

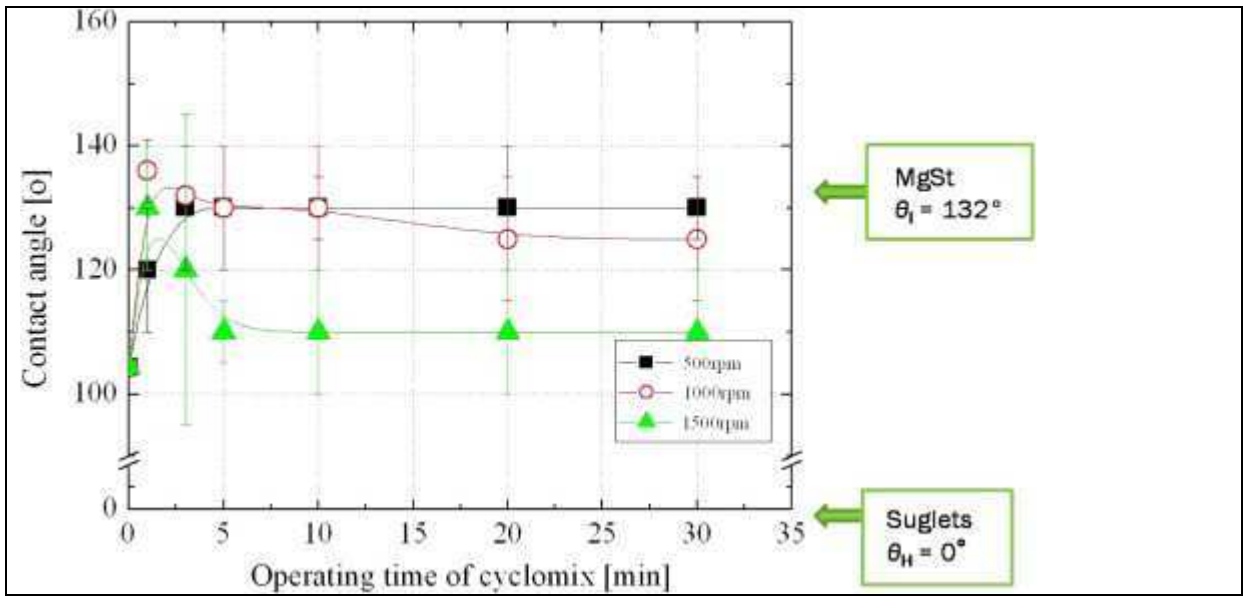

Figure 10: Contact angles as a function of operation time.

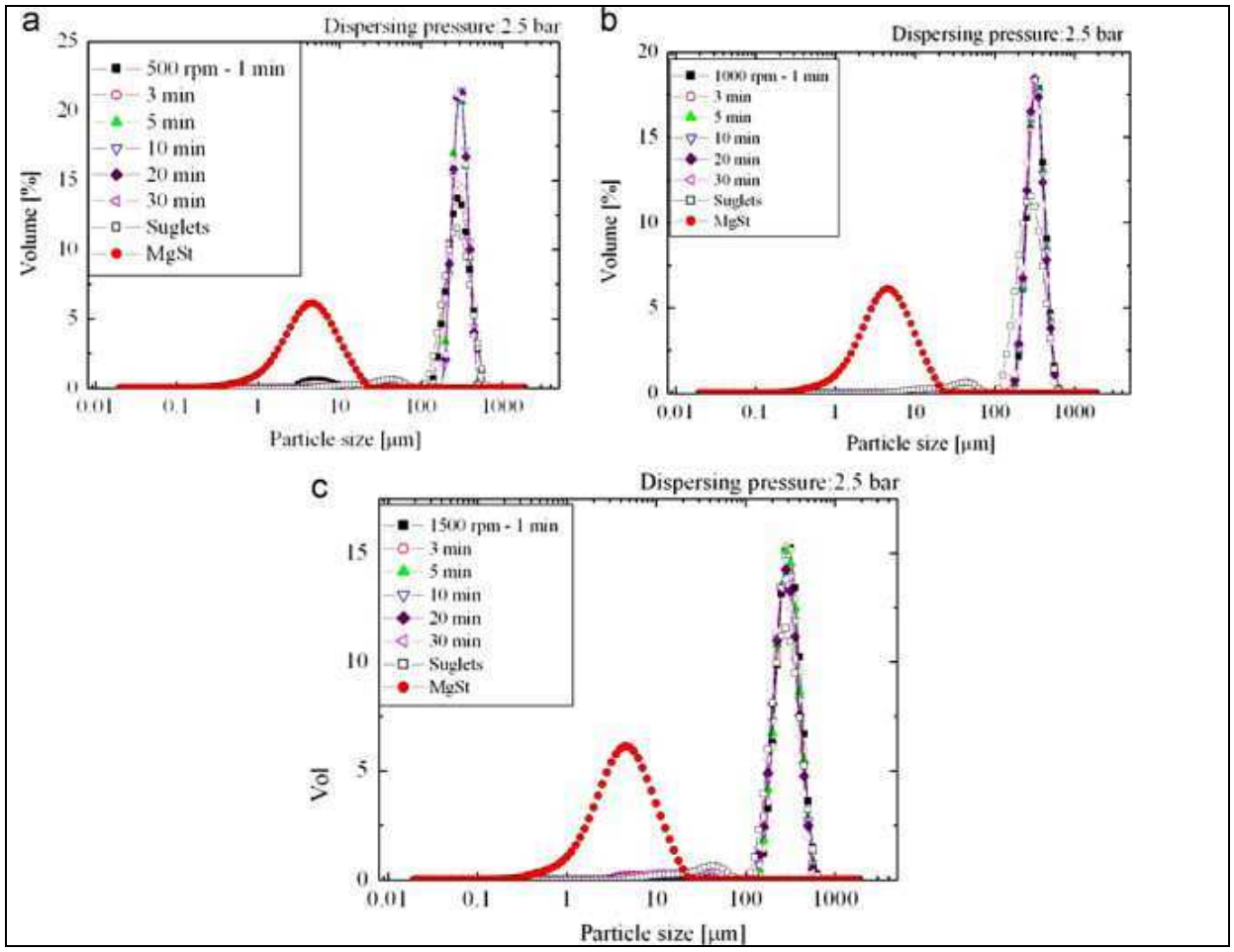

Figure 11: Volume distribution of the particles after operation at 2.5 bar, (a) 500 rpm, (b) 1000 rpm, and (c) 1500 rpm.

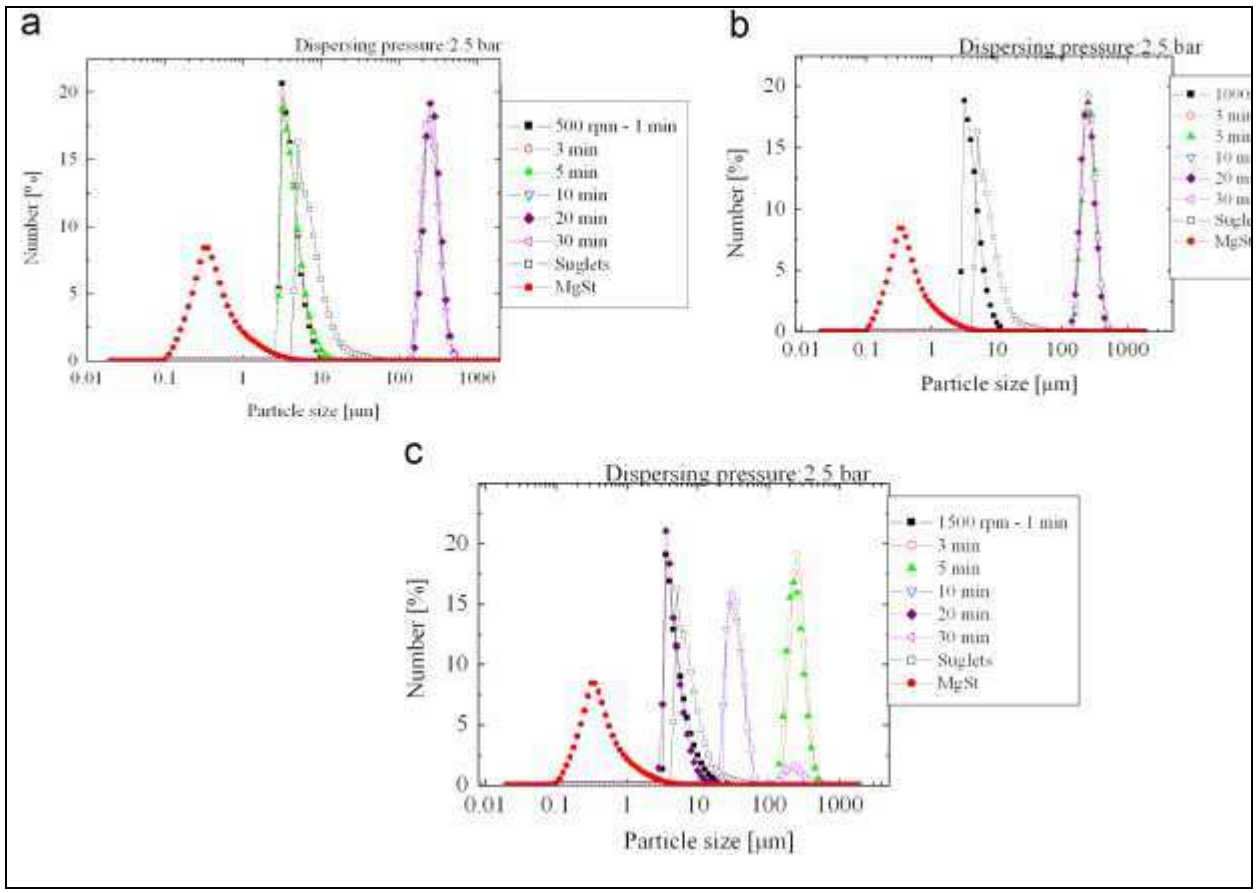

Figure 12: Number distribution of the particles after operation at 2.5 bar, (a) 500 rpm, (b) 1000 rpm, and (c) 1500 rpm

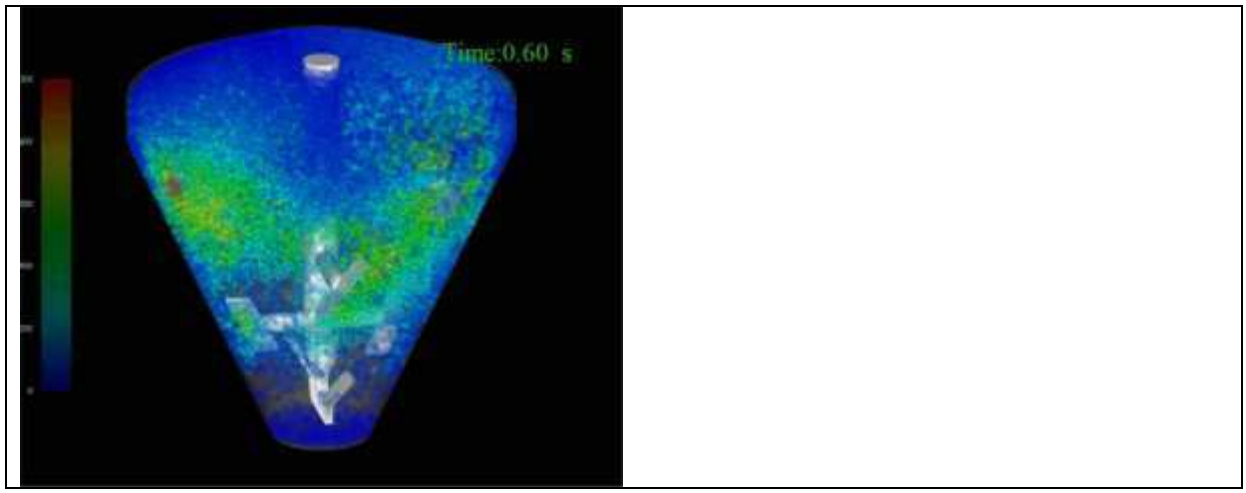

Figure 13: Snapshot of the DEM simulation at 1500 rpm.

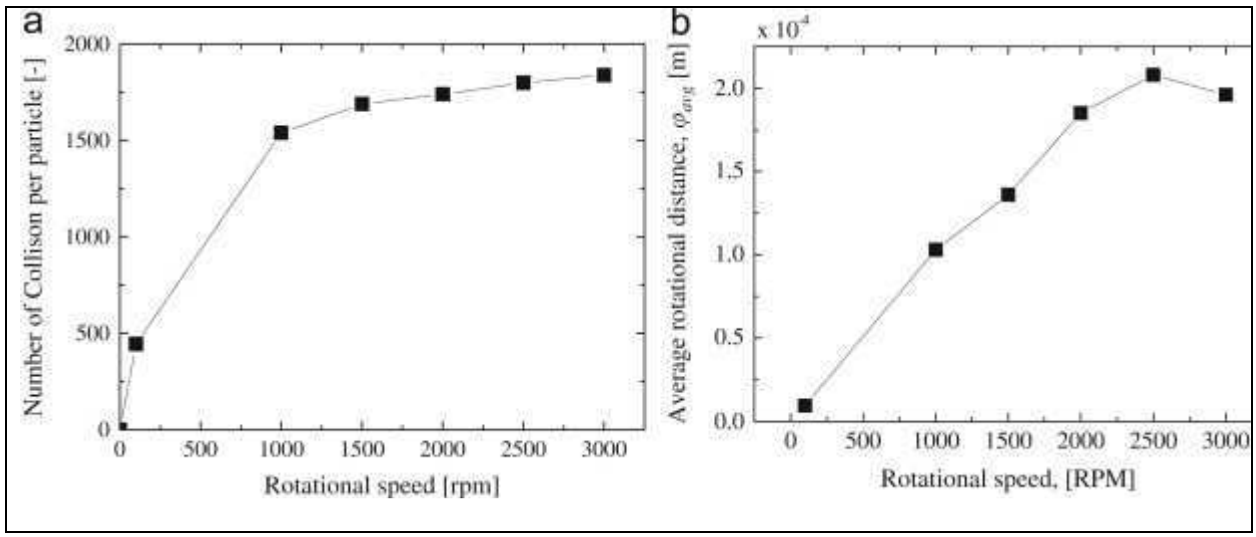

Figure 14: Numerical results, (a) collision number, and (b) rotational distance for each rotational speed.

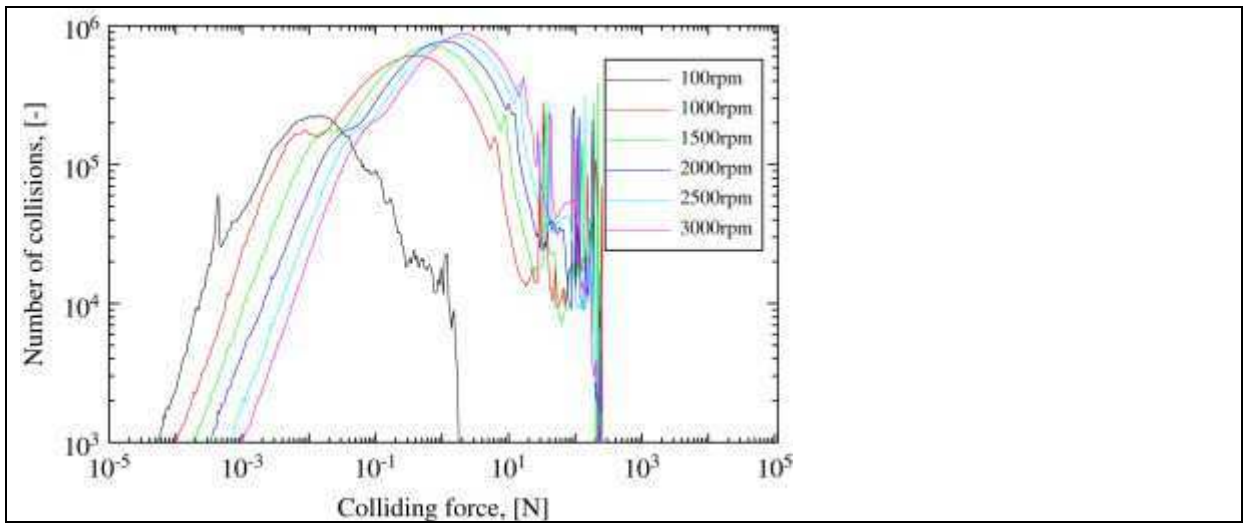

Figure 15: Distribution of the colliding forces of the particles.

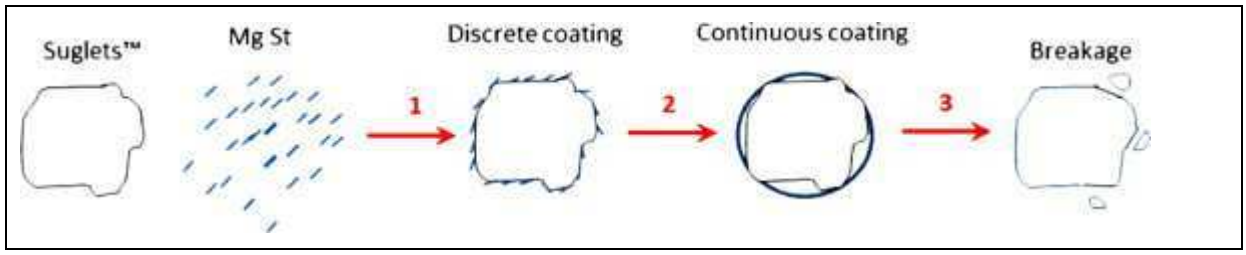

Figure 16: System evolution during dry coating process.